



iJRASET

International Journal For Research in
Applied Science and Engineering Technology



INTERNATIONAL JOURNAL FOR RESEARCH

IN APPLIED SCIENCE & ENGINEERING TECHNOLOGY

Volume: 5 Issue: VIII Month of publication: August 2017

DOI: <http://doi.org/10.22214/ijraset.2017.8278>

www.ijraset.com

Call: ☎ 08813907089

E-mail ID: ijraset@gmail.com

Synthesis and Characterization of ZnO Nanoparticles using Effective of Co Doped

B. Anand and A. Muthuvel

Department Of Physics, Government Arts and Science, Chidambaram -608102

Abstract: *The pure and Co doped ZnO nanoparticles were synthesized by chemical precipitation method at room temperature. The pure and Co doped ZnO nanoparticles have been characterized by X-ray powder diffraction (XRD), Scanning Electron Microscopy (SEM), ultraviolet visible and photoluminescence (PL) spectroscopy, Fourier transform infrared spectroscopy (FTIR). The XRD influence of on crystallite size. The effect of Zn doping with shifting of the bands were observed by UV-Vis spectroscopy and also their optical band gap were determined. The emission spectra and energy band diagram of the pure and Co doped samples were derived from PL spectroscopy. The structural bond vibrations of pure and Co doped ZnO nanoparticles were analyzed by FTIR spectroscopy.*

Keywords: ZnO, Nanoparticles, XRD, UV-visible, PL and FTIR

I. INTRODUCTION

Zinc oxide having interesting physical and chemical properties, together with its cost-effective manufacturing process and abundance in nature, is a promising material for different applications, which has been intensively studied in past decades. The interest in ZnO is fueled and motivated by its excellent properties such as wide direct band gap ($E_g \sim 3.36$ eV at 300 K), high exciton binding energy (60 meV), good piezoelectric characteristics, chemical stability, and biocompatibility which make it a good candidate for diverse application including light-emitting diodes, laser diodes, solar cells, optoelectronic switches, surface acoustic wave devices, hydrogen-storage devices, transparent electrodes, transparent thin-film transistors and sensors [1-4].

These properties makes ZnO attractive in places where high hygiene it's necessary [5]. Therefore, several methods were used to prepare ZnO nanoparticles such as: radio frequency (RF) sputtering process [6], CVD methods [7], pulsed laser deposition [8], spray pyrolysis [9], atomic layer deposition [10], chemical bath deposition [11] or electrodeposition [12]. In sol-gel technique, needs expensive precursors such as alkoxide or organometallic compounds. Forced hydrolysis and hydrothermal synthesis require higher temperatures, pressures and longer reaction time. Microemulsion technique is an important method to preparing large sized monodispersed ZnO nanocrystallites. Among all of these methods, the precipitation technique is an easy way to synthesis the nanoparticles, because of its simple procedure, cheap precursors and easy scalable.

In the present work, pure and Co-doped ZnO nanoparticles were synthesized using precipitation method. The crystalline phase and structure of pure and Co doped ZnO nanoparticles are identified using XRD. The morphology and size of the samples were characterized using Scanning Electron Microscopy (SEM). The optical properties of the nanoparticles were analyzed using, UV-Visible, photoluminescence spectroscopy.

II. EXPERIMENTAL SECTION

A. Materials

Zinc Oxide ($\text{Zn}(\text{NO}_3)_2 \cdot 6\text{H}_2\text{O}$), sodium hydroxide (NaOH), obtained from Nice chemical company. Pvt. Ltd., All the glass wares used in this experimental work were acid washed. The chemical reagents used were analytical reagent grade without further purification. Ultrapure water was used for all dilution and sample preparation. All the chemicals are above 99% purity

B. Methods

In an air atmosphere, Co doped ZnO nanoparticles were synthesized using deionized water. In this experiment, 2.5 g (0.2 M) of ZnO in 50 ml aqueous and Co with different concentrations (0.01–0.03 M. %) were poured into the solution. At room temperature, the mixture was stirred magnetically until a homogeneous solution was obtained. Then, 1 g of 25 ml NaOH was added drop by drop to the above mixture. Precipitate appeared after NaOH injection. The obtained transparent dispersions are purified by dialysis against de-ionized water and ethanol for several times to remove impurities and the products were dried in a hot air oven at 130 °C. The pure ZnO nanoparticles were also synthesized using the same procedure without using doping agent.

C. Characterization Techniques

The optical absorption spectra of the samples were recorded by UV-1650 PC SHIMADZU spectrometer. Using X pert PRO diffractometer with a Cu Ka radiation ($K\alpha = 1.5406 \text{ \AA}$) the X-ray diffraction (XRD) patterns of the powdered samples were recorded. During the recording of the diffractogram, a narrow slit of 0.1 mm was used with a scanning speed of 0.02/s. The size and morphology of the nanoparticles were analyzed using Scanning Electron Microscopy (SEM; JEOL-JSM-5610 LV). Fluorescence measurements were performed on a RF-5301 PC spectrophotometer. The functional groups were determined by a SHIMADZU-8400 Fourier-transform infrared spectrometer in which the IR spectra were recorded in transition mode by diluting the milled powders in KBr and the wavelength between 4000 and 400 cm^{-1} was used to assess the presence of functional groups in pure and Co-doped ZnO.

III. RESULTS AND DISCUSSION

A. Optical Properties

- 1) *UV-Visible Spectroscopy*: The optical properties of pure and Co (0.01–0.03 M. %) doped nanoparticles are examined through UV-visible spectra. From Fig. 1, the all samples have sharp absorption edges in the UV region. The observed absorption edge decreases from 236 to 239 nm with incorporation of ZnO atoms while Co doping results in absorption peak tending toward larger wavelengths. This peak is highly blue shifted compared to the peak value of pure (239 nm).

The band gap values were calculated from absorption data using the following equation 1.

$$E_g = \frac{1240}{\lambda} \quad (1)$$

Where E_g is the optical band gap, and λ is the wavelength corresponding to the relevant absorbance/transmission [13].

The estimated energy gap for the pure ZnO is 5.18 eV, it is increased to 5.25 eV for increasing Co doping level up to 0.01M. %. Further, decrease in the band gap is observed when concentration level increases from 0.02 to 0.03 M.%. The existing blue shift in the band gap is due to the substitution of Co ions into the ZnO lattice. In the case of Co doping, the results reveal that the dopant incorporation leads to decrease of band gap to 5.18 eV. These results are consistent with the reports of others. Since 3d orbital of Co atom is much shallower than 3d orbital of Zn, when a Co atom substitutes Zn in ZnO crystalline lattice, two effects are predictable: (1) strong coupling occurs between d orbital of Co atom and p orbital of O atom, which narrows the direct band gap and (2) Co 3d orbital creates impurity bands above the ZnO valance band [14].

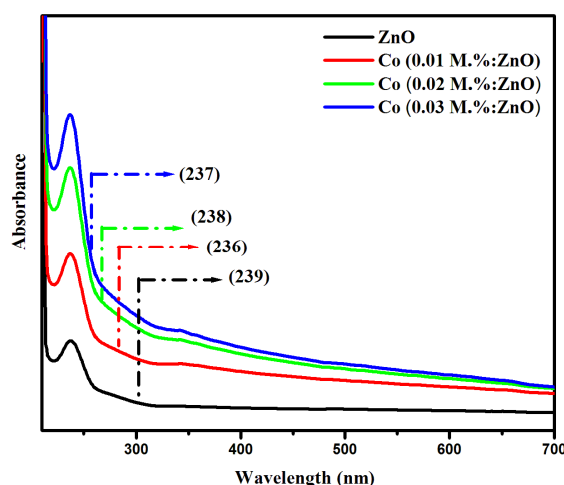


Fig.1. UV-Visible absorption spectrum of pure and Co doped ZnO nanoparticles

B. X-Ray Diffraction Study

Among these doped particles, 0.01 M.% of Co doped ZnO Nanoparticles are having less UV-visible absorption and less crystallite size conformed XRD spectra then pure and other concentrations of 0.02 and 0.03 M.% doped ZnO nanoparticles.

Fig. 2 shows the XRD patterns for ZnO nanoparticles Co doped at 0.01 mol %. As observed, both samples had similar XRD patterns with high crystallinity, corresponding to the ZnO wurtzite hexagonal structure (space group C6mc), according to JCPDS Card No. 36-1451.

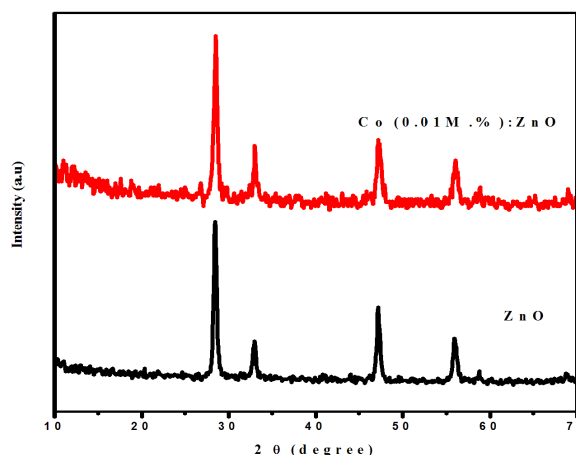


Fig.2. X-ray diffraction patterns of pure and Co-doped ZnO nanoparticles

The calculated crystal sizes, calculated from the Scherrer's formula taking into account the line broadening of the diffracted peak due to the effect of crystal size, are 6.2 nm for the 0.01 mol % samples. No other new phases are observed and intensity while decreased FWHM which confirms the improved crystalline.

The particle sizes were estimated from peak width analysis and using Scherrer equation [15].

$$D_{\text{XRD}} = \frac{K\lambda}{\beta \cos \theta} \quad (2)$$

Where D is the crystallite size, β is the full width half maximum (FWHM), where K is a shape factor (K=0.9 in this work), λ is the wavelength of incident X-rays ($\lambda = 0.15406$ nm).

C. Morphological Studies

- 1) *Scanning Electron Microscopy (SEM)* : The determination of particle size in colloidal solution can be made using dynamic light scattering technique. Particle size distribution with intensity of the optimum concentration for 0.01 M.% of Co doped ceria nanoparticles is observed shown in (Fig.3 a-b).

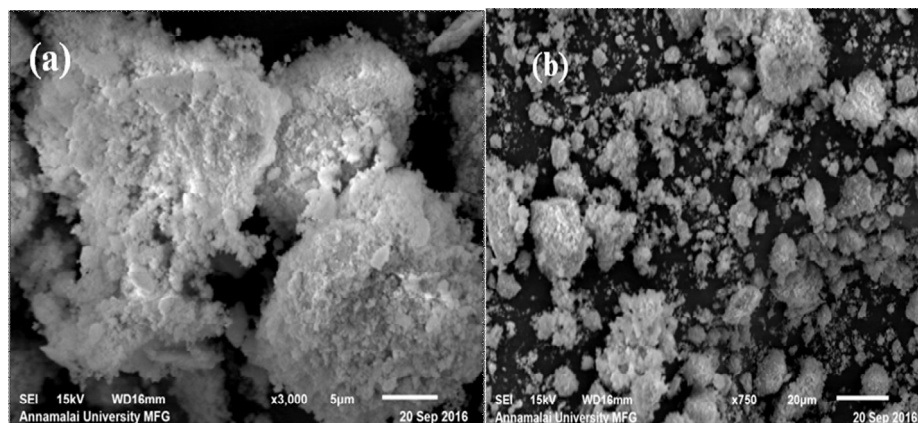


Fig.3. SEM of (a) pure and (b) Co-doped ZnO nanoparticles

These two images show the crystallites with small agglomeration and form aggregates. As seen in the fig 3a & 3b, the distribution of nanoparticles is about 6.2 nm which dictates moderate distribution of the nanoparticles. The observed nanoparticles size is high compared to XRD analysis, since particle aggregations in the nanoparticles are due to water absorption. For this reason, size of the nanoparticles is again confirmed by SEM results.

D. PL Spectroscopy

The PL spectra of Co doped and ZnO nanoparticles with the excitation wavelength of 239 nm are shown in Fig. 3. The emission spectra of 0.01M. % of Co doped ceria were recorded under three different excitation wavelength and their corresponding PL spectra gives wide emission bands which are 340, 396, 437, 468 and 519nm for 239 nm excitation, 468 and 519 nm emission bands for 239 nm excitation and 340 and 396 nm emission bands for 239 nm excitation. The peak appeared around 468 nm belongs to blue emission and the peaks at around 437 nm belong to blue-green emission. However the peak appeared around 519 nm belongs to green emission. The bands at 340 and 396 nm are defect related emissions. The exact reason for this is still controversial. These two bands are believed to be caused by the transition from the level of the ionized oxygen vacancies to the valence band [16].

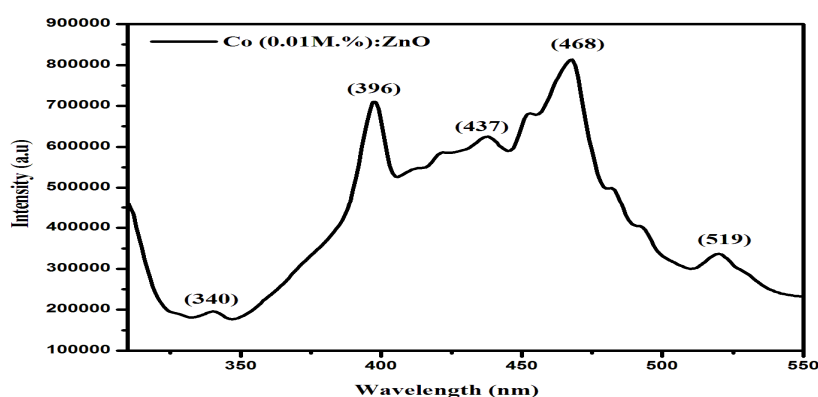


Fig. 4. PL emission spectra of Co doped ZnO nanoparticles.

E. Fourier Transform Infrared Spectroscopy (FTIR)

The IR study gives the information about phase composition as well as the way oxygen is bound to the metal ions. The technique is used to identify the functional groups present in the synthesized material. Fig. 5 shows the IR transmittance spectra of all the samples in the wave number range of 4000-400 cm^{-1} . Broad bands of 3000-3500 cm^{-1} are assigned to O—H stretching at and bending vibrations of H_2O . The bands are located between 2896-2354 cm^{-1} are ascribed to the stretching vibration of CH_3COO^+ groups. The band at 1499 cm^{-1} corresponds to the stretching vibration of CH_2 ethylene group, and those located at 1035 cm^{-1} to the stretching vibrations of CO^- from the organic groups (ethyl, isopropyl and acetic acid). The bands located at 867 cm^{-1} corresponds to the stretching vibrations of the C-C groups. Finally, the strong band located at 435 cm^{-1} corresponds to the Zn—O vibrations [17].

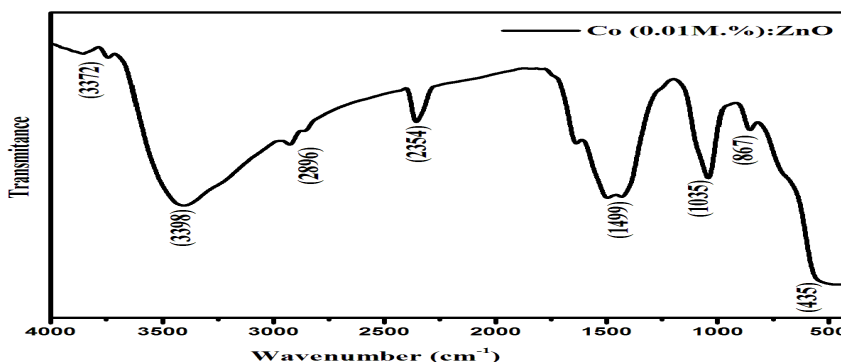


Fig.5. FTIR spectroscopy of Co doped ZnO nanoparticles

IV. CONCLUSIONS

- A. The optical properties of pure and Co (0.01–0.03 M.%) doped nanoparticles are examined through UV–visible spectra. The observed absorption edge decreases from 236 to 239 nm with incorporation of ZnO atoms while Co doping results in absorption peak tending toward larger wavelengths. This peak is highly blue shifted compared to the peak value of pure (239 nm)
- B. The line broadening of the diffracted peak due to the effect of crystal size, are 6.2 nm for the 0.01 mol % samples. No other new phases are observed and intensity while decreased FWHM which confirms the improved crystalline.
- C. These two images show the crystallites with small agglomeration and form aggregates. The observed nanoparticles size is high compared to XRD analysis, since particle aggregations in the nanoparticles are due to water absorption. For this reason, size of the nanoparticles is again confirmed by SEM results.
- D. The peak appeared around 468 nm belongs to blue emission and the peaks at around 437 nm belong to blue–green emission.
- E. The bands located at 867 cm^{-1} corresponds to the stretching vibrations of the C–C groups. Finally, the strong band located at 435 cm^{-1} corresponds to the Zn–O vibrations.

REFERENCES

- [1] U. Ozgür, Y. I. Alivov, C. Liu, A. Teke, M. A. Reshchikov, S. Doğan, V. Avrutin, S.-J. Cho, and H. Morkoç, “A comprehensive review of ZnO materials and devices,” *Journal of Applied Physics*, 98. 4. 041301. 2005.
- [2] A. B. Djurisic, A. M. C. Ng, and X. Y. Chen, “ZnO nanostructures for optoelectronics: Material properties and device applications,” *Progress in Quantum Electronics*, 34. 4. 191–259. 2010.
- [3] C. C. Wu, D. S. Wu, P. R. Lin, T. N. Chen, and R. H. Horng, “Effects of Growth Conditions on Structural Properties of ZnO Nanostructures on Sapphire Substrate by Metal–Organic Chemical Vapor Deposition,” *Nanoscale Research Letters*, 4. 4. 377–384. 2009.
- [4] P. Maddahi, N. Shahtahmasebi, A. Kompany, M. Mashreghi, S. Safaei, and F. Roozban, “Effect of doping on structural and optical properties of ZnO nanoparticles: study of antibacterial properties,” *Materials Science-Poland*, 32. 2. 2014.
- [5] N. Padmavathy and R. Vijayaraghavan, “Enhanced bioactivity of ZnO nanoparticles—an antimicrobial study,” *Science and Technology of Advanced Materials*, 9. 3. 035004. 2008.
- [6] C.-C. Hsiao, K.-Y. Huang, and Y.-C. Hu, “Fabrication of a ZnO Pyroelectric Sensor,” *Sensors*, 8. 1. 185–192. 2008.
- [7] P. Xu and H. Zhuang, “Fabrication and characterisation of multipod ZnO nanostructures by CVD on Al₂O₃-coat Si (111) substrate,” *Micro & Nano Letters*, 6. 12. 985. 2011.
- [8] S. Chakrabarti, B. Doggett, R. O’Haire, E. McGlynn, M. O. Henry, A. Meaney, and J.-P. Mosnier, “Characterization of nitrogen-doped ZnO thin films grown by plasma-assisted pulsed laser deposition on sapphire substrates,” *Superlattices and Microstructures*, 42. 1–6. 21–25. 2007
- [9] N. Lehraki, M. S. Aida, S. Abed, N. Attaf, A. Attaf, and M. Poulain, “ZnO thin films deposition by spray pyrolysis: Influence of precursor solution properties,” *Current Applied Physics*, 12. 5. 1283–1287. 2012.
- [10] G. Scarel, J.-S. Na, B. Gong, and G. N. Parsons, “Phonon Response in the Infrared Region to Thickness of Oxide Films Formed by Atomic Layer Deposition,” *Applied Spectroscopy*, 64. 1. 120–126. 2010.
- [11] Kathalingam, A.; Ambika, N.; Kim, M.R.; Elanchezhyan, J.; Chae, Y.S.; Rhee, J.K. Chemical Bath Deposition And Characterization Of Nanocrystalline ZnO Thin Films. *Materials Science-Poland* 2010, 28, 513-522.
- [12] Márquez, J.A.R.; Herrera, C.M.; Fuentes, M.L.; Rosas, L.M. Effect Of Three Operating Variables On Degradation Of Methylene Blue By ZnO Electrodeposited: Response Surface Methodology, *International Journal Of Electrochemical Science* 2012, 7, 11043-11051.
- [13] H.-I. Chen and H.-Y. Chang, “Synthesis of nanocrystalline cerium oxide particles by the precipitation method,” *Ceramics International*, 31. 6. 795–802. 2005.
- [14] K.-S. Ahn, T. Deutsch, Y. Yan, C.-S. Jiang, C. L. Perkins, J. Turner, and M. Al-Jassim, “Synthesis of band-gap-reduced p-type ZnO films by Cu incorporation,” *Journal of Applied Physics*, 102. 2. 023517. 2007.
- [15] B. D. Cullity and R. Smoluchowski, “Elements of X-Ray Diffraction,” *Physics Today*, 10. 3. 50–50. 1957.
- [16] W. M. Kwok, A. B. Djurišić, Y. H. Leung, W. K. Chan, and D. L. Phillips, “Time-resolved photoluminescence from ZnO nanostructures,” *Applied Physics Letters*, 87. 22. 223111. 2005.
- [17] M. Vafaei and M. S. Ghamsari, “Preparation and characterization of ZnO nanoparticles by a novel sol–gel route,” *Materials Letters*, 61. 14–15. 3265–3268. 2007.



10.22214/IJRASET



45.98



IMPACT FACTOR:
7.129



IMPACT FACTOR:
7.429



INTERNATIONAL JOURNAL FOR RESEARCH

IN APPLIED SCIENCE & ENGINEERING TECHNOLOGY

Call : 08813907089  (24*7 Support on Whatsapp)